

Beam splitter geometry for Iron-Pnictide materials

Abhisek Bag^{1,2,*} and Saptarshi Mandal^{1,2,†}

¹*Institute of physics, Bhubaneswar 751005, Odisha, India*

²*Homi Bhabha National Institute, Mumbai 400 094, Maharashtra, India*

(Dated: September 13, 2021)

We consider a Cooper pair beam splitter for Iron-Pnictide S_{+-} superconductor and calculate the entangled electron-hole current. We investigate the interplay of various physical parameters such as doping at electron and hole pockets as well as non-zero nesting between the electron and hole pocket. In general we find that the presence of magnetic ordering decreases the beam splitter current by a factor of one hundred in comparison to pure BCS superconductor in two dimensions. For equal size electron-hole pocket and zero nesting we find that the beam-splitter current in general depends non-monotonically on the chemical potentials at electron and hole pockets. For non-zero nesting at a fixed chemical potential the current also varies non-monotonically with nesting vector $|\mathbf{q}|$. This non-monotonous or oscillatory behavior is attributed to inter-dependency of density of states at hole and electron pocket due to coupling between the electron and hole pockets. Our finding can be useful in experimental determinations or verification of co-existence phase in Iron-Pnictide superconductors and has potential applications in realizing quantum gates or switches.

I. INTRODUCTION

One of the fundamental aspect of quantum mechanics is the superposition principle which dictates that a quantum mechanical system can be described by a linear superposition of many orthogonal wave function [1]. This superposition principle yields an entanglement or correlations between different parts of the system. In recent times this fundamental aspect has been investigated in detail to construct entangled states having specific properties with application in teleportation, cryptology etc [2]. To realize such entangled states many protocols have been proposed involving various mesoscopic system such as quantum dots, superconducting qubits etc [3–5]. However after preparing such entangled state one needs to confirm that the state is robust against decoherence [7, 8]. It is an well known fact that various condensed matter system act as a resource of such entangled many body states naturally. The existence of such entangled states is ubiquitous in various condensed matter systems such as the Cooper pairs in superconductivity [9], ground state wave-function for quantum spin liquid [10, 11], resonating valence bond states [12] for certain magnetic systems etc.

Starting from the celebrated EPR paradox [13] and culminating in Bell's inequality [14, 15], entanglement is now an experimentally established reality [16–18]. In view of identifying such entangled states in the context of superconductivity, a Cooper pair beam splitter arrangement has been proposed for the first time in Ref [19] and later on other system [20, 21]. In these study it is proposed that the participating electrons and holes can be collected at two different leads after passing through two quantum dots kept at spatially suitable distance. The collected

electron and hole maintain their state of initial correlation or entanglement. Recently such studies has been extended to graphene [22] where an proximity induced superconductivity has been considered. There the authors have shown that the beam splitter current is increased in magnitude in comparison to an ideal BCS superconductor in two dimensions. However the superconductivity in single layer graphene is not realized till now and the superconductivity in conventional BCS superconductor is realized at very low temperature limiting its practical application. Thus it motivates us to look for other system where such entangled beam splitter can be realized with naturally occurring superconductivity at high temperatures enabling us for practical applications.

In this study we have investigated the consequences of beam splitter arrangement for Iron-pnictide superconductors. We are motivated by the fact that this system is realized at quite high temperature for example at $\sim 50\text{K}$ for 1111- and 122- type systems [23] thus providing relatively easier practical realisation. Apart from this fact, the Iron-pnictide system is well known for the co-existence of superconducting order as well as magnetic order [23–26]. This aspect is quite remarkable in the sense that unlike conventional BCS superconductor, in Iron-pnictide superconductivity does not get destroyed by the application of moderate magnetic field easily. In fact we have found that the copper pair beam splitter current depends on the relative magnitude of chemical potential, superconducting gap and the magnetic order parameter to a large extent. We have also seen that unlike before, the beam current can be monotonically decreasing or an oscillating one depending on the relative shapes of the electron and hole pocket as well as values of chemical potential at electron and hole pocket respectively. This may give an added advantage towards practical application [23] of Iron-pnictide beam splitters. Our plan of presentation is the following. In section II we review the basics of Iron-pnictide superconductors, its model hamiltonian and spectrum. After this, in section III we present

* abhisek.b@iopb.res.in

† saptarshi@iopb.res.in

our model scheme of realising beam splitter current in detail by calculating the entangled beam splitter current in its full form for the Iron-pnictide system. We also enumerate all the assumption and approximation needed for such calculation. In section IV, we present graphically the beam splitter current vs the distance between the two leads for various parameter values of the system such as chemical potential at electron and hole pocket, perfect and non-zero nesting etc. Finally we conclude in section V by summarising our results with a discussion.

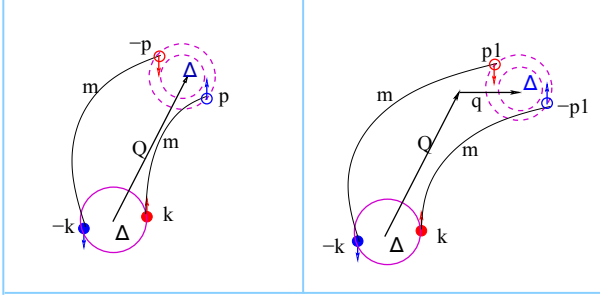


FIG. 1. In the above the solid circles denote hole pocket and the dashed circles denote electron pocket. The black lines connecting fermions from electron and hole pocket is responsible for magnetic ordering in the system. The left panel shows the case of perfect nesting and the right panel shows a non-zero nesting (finite \mathbf{q}). Δ denotes the superconducting gap at the electron and hole pocket.

II. MODEL

In FeAs, the relevant tight binding model which describes the superconductivity contains an itinerant electron system of two electronic orbitals due to two Fe atoms in a unit cell. The hybridization between the orbitals are such that it leads to a hole pockets centred at $(0,0)$ and an electron pocket centred at π, π in the folded zone scheme [27, 28]. Following earlier notations[27] we denote the fermions near $(0,0)$ by usual ‘ c ’ operator and for fermions near (π, π) by ‘ f ’. The model Hamiltonian can be written as follows,

$$H = H_0 + H_\Delta + H_m. \quad (1)$$

In the above H_0 denotes the non-interacting part of electron and hole pockets. H_Δ denotes superconducting pairing interaction and H_m signifies the magnetic pairing interaction. The details of these three terms are given below [28],

$$H_0 = \sum_k \epsilon_c(k) c_{k\alpha}^\dagger c_{k\alpha} + \sum_{k'} \epsilon_f(k') f_{k'\alpha}^\dagger f_{k'\alpha} \quad (2)$$

$$\epsilon_c(k) = \mu_c - \frac{k^2}{2m_c}, \quad \epsilon_f(k) = \frac{k_x^2}{2m_{fx}} + \frac{k_y^2}{2m_{fy}} - \mu_f. \quad (3)$$

In the above ‘ k ’ appearing in ‘ c ’ is measured from the center of Brillouine zone and for ‘ f ’ fermion k' is measured from (π, π) . Note that we have taken an Isotropic

mass at electron pocket and anisotropic mass at hole pocket for general model. For simplicity we would be assuming an isotropic mass for electron pocket as well i.e $m_{fx} = m_{fy} = m_f$. The superconducting pairing terms and the magnetic interactions are given by,

$$H_\Delta = \frac{1}{2} \sum_{k,p} V_{\alpha\beta\beta'\alpha'}^{cf}(k,p) (c_{k\alpha}^\dagger c_{-k\beta}^\dagger f_{-p\beta'} f_{p\alpha'} + f_{k\alpha}^\dagger f_{-k\beta}^\dagger c_{-p\beta'} c_{p\alpha'}), \quad (4)$$

$$H_m = -\frac{1}{4} \sum_{p'-p=k'-k} V_{\alpha\beta\beta'\alpha'}^{SDW}(p'p : kk') (f_{p'\alpha}^\dagger c_{p\beta} c_{k\beta'}^\dagger f_{k'\alpha'} + f_{-p\alpha}^\dagger c_{-p\beta} c_{-k\beta'}^\dagger f_{-k'\alpha'}). \quad (5)$$

In the above, Eq. 4 describes the effective pairing interactions in the Iron-pnictide system which arises due to the inter-band hopping between electron and hole band [27]. The magnetic interactions as denoted in Eq. 5 comes from the inter-band density-density interactions. The pairing interaction $V_{\alpha\beta\beta'\alpha'}^{cf}(k,p)$ and the magnetic interaction $V_{\alpha\beta\beta'\alpha'}^{SDW}(p'p : kk')$ have the representation,

$$V_{\alpha\beta\beta'\alpha'}^{cf}(k,p) = V_{k,p}^{SC} ((i\sigma^y)_{\alpha\beta} (i\sigma^y)_{\beta'\alpha'}^\dagger) \quad (6)$$

$$V_{\alpha\beta\beta'\alpha'}^{SDW}(p'p : kk') = V_{p'p:kk'}^{SDW} \sigma_{\alpha\beta} \cdot \sigma_{\beta'\alpha'}^\dagger. \quad (7)$$

Following conventional way, we define the superconducting pairing order parameters and magnetic order parameter as follows,

$$\Delta_c(k)_{\alpha\beta} = (i\sigma^y)_{\alpha\beta} \sum_p V_{kp}^{SC} (i\sigma^y)_{\beta'\alpha'}^\dagger \langle f_{-p\beta'} f_{p\alpha'} \rangle \quad (8)$$

$$\Delta_f(k)_{\alpha\beta} = \sum_p V_{kp}^{SC} (i\sigma^y)_{\beta'\alpha'}^\dagger \langle c_{-p\beta'} c_{p\alpha'} \rangle \quad (9)$$

$$(m_q)_{\alpha\beta} = -\frac{V^{SDW}}{2} \sum_p \sigma_{\alpha\beta} \cdot \sigma_{\beta'\alpha'}^\dagger \langle c_{p\beta'}^\dagger f_{p+q\alpha'} \rangle \quad (10)$$

We use the above definitions to perform a meanfield decomposition of the four fermion interactions as given in Eq. 4 and Eq. 5. The resulting Hamiltonian obtained is written in the following matrix form,

$$H = \sum_{k\alpha\beta} \bar{\Psi}_{k\alpha} \hat{H}_{\alpha\beta} \Psi_{k\beta} - 2 \frac{\Delta_c \Delta_f}{V_{SC}} + 2 \frac{m_{\alpha\beta}^+ m_{\alpha\beta}}{V_{SD}}, \quad (11)$$

where the four component Nambu spinor is, $\bar{\Psi}_{k\alpha} = (c_{k\alpha}^\dagger, c_{-k\alpha}, f_{p\alpha}^\dagger, f_{-p\alpha})$ and the Hamiltonian matrix $\hat{H}_{\alpha\beta}$ has the form,

$$\hat{H}_{\alpha\beta} = \begin{pmatrix} \epsilon_c(k)_{\alpha\beta} & \Delta_c(k)_{\alpha\beta} & m_{q\alpha\beta}^* & 0 \\ \Delta_c(k)_{\alpha\beta} & -\epsilon_c(k)_{\alpha\beta} & 0 & -m_{q\alpha\beta}^* \\ m_{q\alpha\beta} & 0 & \epsilon_f(q)_{\alpha\beta} & \Delta_f(q)_{\alpha\beta} \\ 0 & -m_{q\alpha\beta} & \Delta_f(-q)_{\alpha\beta} & -\epsilon_f(-q)_{\alpha\beta} \end{pmatrix}. \quad (12)$$

Notice that in the above equation, we have accounted for two different kind of magnetic order parameter with the following definitions,

$$\alpha = \beta \implies m_{\alpha\beta} = m_1 \ \& \ \alpha \neq \beta \implies m_{\alpha\beta} = m_2. \quad (13)$$

Following earlier study [27, 28] we choose $m_1 = m, m_2 = 0$ in our study without loss of generality. One can easily obtain the spectrum after diagonalizing the 8×8 matrix in Eq. 12, the detail expressions for the eigenvalues are given in Appendix B. We obtain the ground state energy by filling the negative energy eigenstates which correspond the vacuum of new Bogoliubov quasi particles. Along with the constant terms the ground state energy can be written as,

$$E_{min} = -\frac{1}{\sqrt{2}}[\sqrt{(A_k + \sqrt{B_k})} + \sqrt{(A_k - \sqrt{B_k})}] - 2\frac{\Delta_c\Delta_f}{V_{SC}} + 2\frac{m^2}{V_{SD}}. \quad (14)$$

In the above A_k and B_k are functional of $\epsilon_c(k), \epsilon_f(p), \Delta_c, \Delta_f, m$ and their detail expressions are given in Appendix B. We calculate the meanfield order parameter by minimizing the above ground state energy and solving the resulting self-consistent equation. Once the meanfield order parameter values are obtained we use them to calculate the beam splitter current.

III. MODEL FOR BEAM SPLITTER GEOMETRY

Having described the basic model of superconductivity in Iron-Pnictides we now elaborate on our beam splitter arrangement. Our idea of entangled cooper pair splitter is similar to the seminal work of [19] where for the first time an outline of cooper pair entangled beam splitter arrangement is introduced. In Fig. 2, we presented a schematic diagram of entangled beam-splitter arrangement. It is expected that electrons in a superconducting pair in an iron-pnictide material will be tunneling through two spatially separated quantum dots where each quantum dot allows one electron (among the two participating electron in an superconducting pair). This is expected to happen once the quantum dots are kept in the coulomb blocked regime such that it is energetically unfavorable to accommodate two electron at the same quantum dot. Finally once two spatially separated electrons enter into two separate quantum dots, they are collected by two fermi liquid leads (represented by L_1 and L_2 in Fig. 2). However to realize such entangled electrons to be separated the chemical potentials of the superconducting materials (μ_s), quantum dots (ϵ_1 and ϵ_2) and also the leads (μ_1 and μ_2) has to be kept in certain condition. While the chemical potentials at the two fermi liquid leads can be kept equal generally, the chemical potentials of the two quantum dots should be such that $\epsilon_1 + \epsilon_2 = 2\mu_s$ corresponding a two particle Breit-Wigner

resonance [29]. The transport of two entangled pair from the quantum dots to the leads can be achieved by applying a bias voltage $\Delta\mu = \mu_s - \mu_l$.

It is natural to expect that once the electrons tunnels from the superconductor to quantum dots, they interact with the already existing electrons at the quantum dots and this might lead to loss of decoherence between the two separated electrons. One way to avoid this is to work in the co-tunneling regime where the number of electrons in the quantum dots are fixed and also the resonant level ϵ_1, ϵ_2 are not occupied. The probability of interaction can also be reduced if the entered electrons spend less time in the quantum dots and this can be achieved by having $|T_{SD}| < |T_{DL}|$. Also the temperature of the superconductor and the quantum dots should be such that $\Delta_\mu > K_B T$ as this will ensure that the stationary occupation due to the coupling to leads is exponentially small. The complete Hamiltonian for the

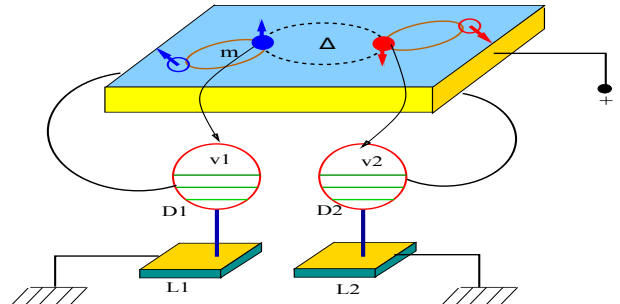


FIG. 2. Cartoon picture of Cooper Pair Beam Splitter Setup for Iron-pnictide superconductor. The blue rectangular slab with yellow border represents the superconductor and a Bogoliubov quasiparticle has been drawn schematically on it. The two filled circles represent fermions participating in superconducting order parameter Δ and the magnetic order is represented by the coupling between one filled circle and one empty circle. The superconducting slab is connected to two quantum dots (D1 and D2) by black lines. Each quantum dot is finally connected to fermi leads L_1 or L_2 .

proposed beam splitter devices thus involves the intrinsic Hamiltonian of the Iron-pnictide materials, two quantum dots and two fermi liquid quantum leads. In addition to the intrinsic Hamiltonian, it also involves the tunneling Hamiltonians between the superconductor and the quantum dots and between the quantum dots and the leads. The complete Hamiltonian represented by H_C for the beam splitter set up thus becomes,

$$H_C = H_S + \sum_l H_{D,l} + \sum_l H_{L,l} + H_{SD} + H_{DL}. \quad (15)$$

In the above the first three terms indicate the intrinsic Hamiltonian of superconducting material, quantum dots and lead respectively. Henceforth the subscript S, D, L will be used for the superconductor, quantum dots and the leads respectively. ' l ' denotes the number of leads and quantum dots which can take values 1 and 2. The term H_{SD} and H_{DL} denotes the tunneling Hamiltonian from

superconductor to quantum dots and quantum dots to leads respectively. Below we give in detail the complete expressions of each terms in Eq. 15.

$$H_S = \sum_{k\sigma} [E_{kq-} \gamma_{kq\sigma}^{1+} \gamma_{kq\sigma}^1 + E_{kq+} \gamma_{kq\sigma}^{2+} \gamma_{kq\sigma}^2] + \mathcal{E}_0 \quad (16)$$

$$H_{Dl} = \sum_{\sigma,l} \epsilon_l d_{l\sigma}^+ d_{l\sigma} + U n_{l\sigma} n_{l-\sigma} \quad (17)$$

$$H_{Ll} = \sum_{k\sigma} \epsilon_k a_{lk\sigma}^+ a_{lk\sigma} \quad (18)$$

$$H_{SD} = \sum_{l\sigma,i} g_i T_{SD}^i d_{l\sigma}^+ \Psi_\sigma^i(r_l) + h.c \quad (19)$$

$$H_{DL} = \sum_{lk\sigma} T_{DL} a_{lk\sigma}^+ d_{l\sigma} + h.c \quad (20)$$

In the above $E_{kq\pm}$ denotes the energy of Bogoliubov quasi-particle excitations which are represented by $\gamma_{kq\sigma}^1$ and $\gamma_{kq\sigma}^2$ respectively. \mathcal{E}_0 denotes the condensation energy and does not effect the beam-splitter arrangements. ϵ_l denotes the energy levels of quantum dots and U signify the interaction energy if a given energy level of the quantum dot is occupied with two electrons of opposite spins. ϵ_k describes the energy of the Bloch states of fermi liquid leads. T_{SD}^i is the tunneling amplitude between superconductor and i 'th quantum dots and Ψ^i represents a state of an electron/hole arriving at i 'th quantum dot. g_1 and g_2 can take value 0 or 1 depending on which kind of quasi-particle is taking part in the Andreev process. We note that $g_1 \neq g_2$ signifying that two types of quasi particles can not be present simultaneously in a pair of dots. Lastly T_{DL} denotes the tunneling amplitude between quantum dots and fermi liquid leads.

A. Current: via different dots

Having provided a brief introduction on Iron-pnictide system in Sec. II and the beam-splitter set up in detail in Sec. III, we now outline the important steps in evaluating beam-splitter current which are finally measured at the fermi liquid leads. The current due to electrons coming from superconductor and finally reaching to lead via quantum dots are represented by [19]

$$I = 2e \sum_{f,i} W_{f,i} \rho_i, \quad (21)$$

where $W_{f,i} = 2\pi | \langle f | T_{\epsilon_i} | i \rangle |^2 \delta(\epsilon_f - \epsilon_i)$ is transition rate from an initial state of electron $|i\rangle$ to a final state $\langle f|$ and ρ_i denotes the electron density. Here $T(\epsilon_i)$ is the on-shell transmission matrix and is given by [30],

$$T(\epsilon_i) = H_T \frac{1}{(\epsilon_i + i\eta - H)} (\epsilon_i - H_0). \quad (22)$$

In the above H_0 denotes the Hamiltonian for superconductor ($H_0 = H_S$) and H_T denotes the successive tunneling from superconductor to quantum dots and subsequently from quantum dots to leads. $H = H_C$, is the

total Hamiltonian. As $H_T \ll H_0$, we can expand the denominator in appropriate power series and we obtain in $\eta \rightarrow 0$ limit,

$$T(\epsilon_i) = H_T + H_T \sum_{n=1 \rightarrow \infty} \left(\frac{H_T}{(\epsilon_i + i\eta - H_0)} \right)^n. \quad (23)$$

We note that $\langle f | T(\epsilon_i) | i \rangle$ denotes two step processes such that $\langle f | T | i \rangle = \langle f | T' | f' \rangle \langle f' | T'' | i \rangle$ where T'' denotes the tunneling from superconductor to quantum dots and T' denotes the tunneling from quantum dots to leads. The expressions for T' and T'' are obtained as,

$$T'' = \frac{1}{i\eta - H_0} H_{SD} \frac{1}{i\eta - H_0} H_{SD} \quad (24)$$

$$T' = H_{DL} \sum_{n=0 \rightarrow \infty} \left(\frac{H_{DL}}{i\eta - H_0} \right)^{2n+1}. \quad (25)$$

We note that $|i\rangle = |0\rangle_S \otimes |0\rangle_D \otimes |\mu_l\rangle_l$ where the subscript S, D, l are used to denote the initial states of superconductor, quantum dots and leads respectively. The states $|f\rangle = |LL\rangle, |f'\rangle = |DD\rangle$ denotes the final states of leads and quantum dots respectively which are due to arrival of electrons from superconductor and hence represents a state with higher number of electrons and can be written as,

$$|f\rangle = \frac{1}{\sqrt{2}} (a_{1p\uparrow}^+ a_{2q\downarrow}^+ - a_{1p\downarrow}^+ a_{2q\uparrow}^+) |i\rangle, \quad (26)$$

$$|f'\rangle = \frac{1}{\sqrt{2}} (d_{1\uparrow}^+ d_{2\downarrow}^+ - d_{1\downarrow}^+ d_{2\uparrow}^+) |i\rangle. \quad (27)$$

Taking into account the orthogonality of states of different occupation numbers and momentum conservation, we obtain,

$$\langle f | T' | f' \rangle = \langle i | a_{2q\downarrow} a_{1p\uparrow} T' d_{1\uparrow}^+ d_{2\downarrow}^+ | i \rangle. \quad (28)$$

We now turn to simplify $\langle f' | T'' | i \rangle = \frac{1}{\sqrt{2}} \langle i | (d_{2\downarrow} d_{1\uparrow} - d_{2\uparrow} d_{1\downarrow}) T'' | i \rangle$, which denotes Andreev process. It may happen that in the process of transport one electron with a particular spin(say up) arrives at the quantum dot from the superconductor but an electron with opposite spin(say down) may travel forward from the same dot to the lead but we forbid that process. We want processes such as $|SS\rangle \rightarrow |DS\rangle \rightarrow |DD\rangle$ and $|SS\rangle \rightarrow |SD\rangle \rightarrow |DD\rangle$. Such that entangled pair of electrons from the superconductor(SS) get transported to dot(DD) and move forward to the lead, because we avoid spin flipping. Where, $|SD\rangle = \gamma_{k\sigma}^+ d_{l-\sigma}^+ |i\rangle$. We ensure that $H_{S_1 D_1}$ selects one electron of the entangled pair to dot 1 & $H_{S_2 D_2}$ selects the other electron of the entangled pair to dot 2. A little algebra gives us the following expression,

$$\langle f' | T'' | i \rangle = \frac{1}{\sqrt{2}} \frac{2(T_{SD})^2}{\epsilon_1 + \epsilon_2 - i\eta} \sum_{kl} \frac{U_{kq}^l}{E_{kq}^l}, \quad (29)$$

where l can be 1 and 2 number of available quasiparticles in the system. The final expression for the current is given below,

$$I = \frac{2e\gamma(T_{SD})^4}{(\epsilon_1 + \epsilon_2)^2 + \frac{\gamma^2}{4}} \times \left| \sum_{izp} (u_{iz}^p u_{i+1z}^p - u_{i-z}^p u_{i+1-z}^p) \cos(\bar{k} \cdot \delta \bar{r}) / E_z^i \right|^2. \quad (30)$$

In the above $\gamma = \sum \gamma_{lead}$; $lead = 1, 2$ and $\gamma_{lead} = 2\pi T_{DL}^2$. Also $i = 1, 3$; $p = c, f$; $z = k, k'$; are the possible values for summation. The detailed expressions for u values are given in the appendix. The above expression for current is evaluated numerically and plotted against $k_F \delta r$ for different values of system parameters such as doping at electron and hole pocket, nesting vectors etc in the next section.

IV. NUMERICAL RESULTS

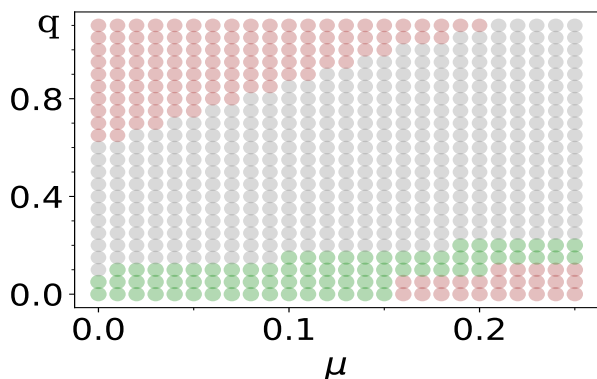


FIG. 3. The phase diagram in \mathbf{q} - μ plane. The region filled with green filled circle denotes magnetic phase. The pink colored region denotes superconducting phase and grey colored region is the co-existence phase where superconducting and magnetic order co-exist.

We numerically solve the self consistent equations for order parameters to get the corresponding values and used them to compute the current as given in Eq. 30. Before presenting our results for the beam-splitter current we briefly discuss the phase diagram in \mathbf{q} vs μ plane where \mathbf{q} is the nesting vector and μ denotes the amount of doping in the hole or electron pocket. In Fig. 3 we have plotted the phase diagram obtained after numerically solving the self-consistent equations as described in Sec.II. The salient feature of the phase diagram is that the co-existence phase which is the most interesting aspect of Iron-pnictide superconducting system exists for specific values of \mathbf{q} and μ . For example, to get the co-existence phase a finite nesting is needed. Now we proceed to discuss the beam splitter current evaluated in different parameter regime.

A. Comparison of beam splitter current for electron doped vs hole doped

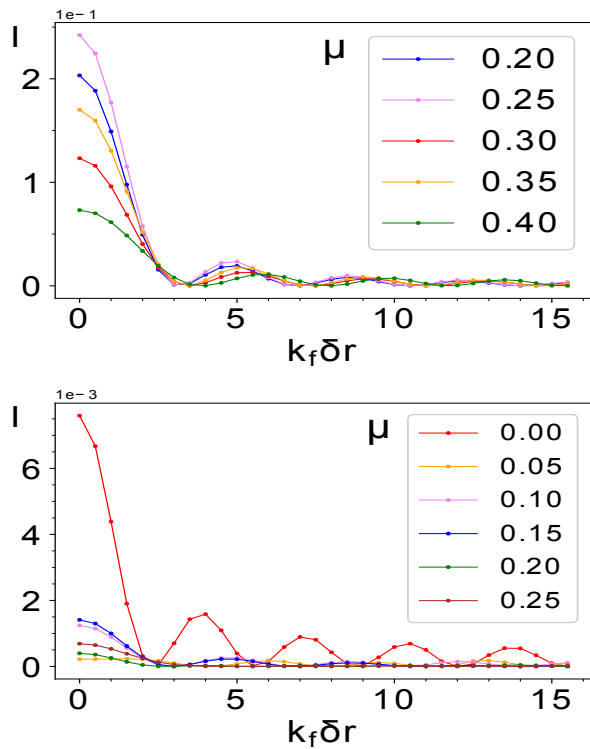


FIG. 4. Beam splitter current is plotted for identical shapes of electron and hole pocket for different chemical potential. Here the chemical potential μ refers both the electron and hole doping. In the upper panel we plotted current for perfect nesting $\mathbf{q}=\mathbf{0}$ and in the lower panel we have plotted current for finite nesting.

Here we discuss how the current varies with distance between the leads when the chemical potential at hole and electron pocket are varied independent of each other. First we discuss what happens when there is perfect nesting such that $\mathbf{q} = \mathbf{0}$. In this case we note that there is no co-existence phase and magnetic order parameter does not exist. As a result there is no such entanglement between the hole and electron pocket though the superconducting gap in hole pocket is determined by the electrons at electron pocket and vice-versa according to Eq. 8 and Eq. 9. Throughout this investigation we have taken identical shape of the hole and electron pocket which is circular in our case, for simplicity. In the upper panel of Fig. 4 we plotted the current when the nesting vector $|\mathbf{q}|$ is zero and in the lower panel we have plotted for a finite nesting vector \mathbf{q} . Due to symmetry the beam current does not depend on the nature of doping whether it is electron doped or hole doped. The chemical potential μ in Fig. 4 represents either μ_c or μ_f when μ_f and μ_c is zero respectively. This is consistent with the symmetry of the system. In both the cases, however, the current is non-linear for a given value of $k_F \delta r$. For example when

μ is increased from 0.2 to 0.25 in the upper panel of Fig. 4, we find an increase in current but further increase in μ to 0.4 causes a decrease in current for perfect nesting. Similar observation holds for finite nesting as well. The main difference between the upper and lower panel of the Fig. 4 is that the magnitude of current is decreased by two decimal magnitude for finite \mathbf{q} . Noting that a finite \mathbf{q} represents a co-existence phase having magnetic and superconducting order parameter both, it can be concluded that existence of magnetic order parameter is the main reason behind this decrease of current. However the property which is common in both the cases is that current is oscillatory at a given $k_f \delta r$ with respect to varying μ . The reason of oscillation is that though they behave like two independent copies of BCS system, the superconducting pairing amplitude at hole pocket is determined by the electron pocket and vice versa. This interdependence causes the oscillations of density of states [28] and hence the beam current behaves in a non-linear way with respect to doping and nesting vector \mathbf{q} .

B. Variations of beam splitter current with respect to nesting vector \mathbf{q}

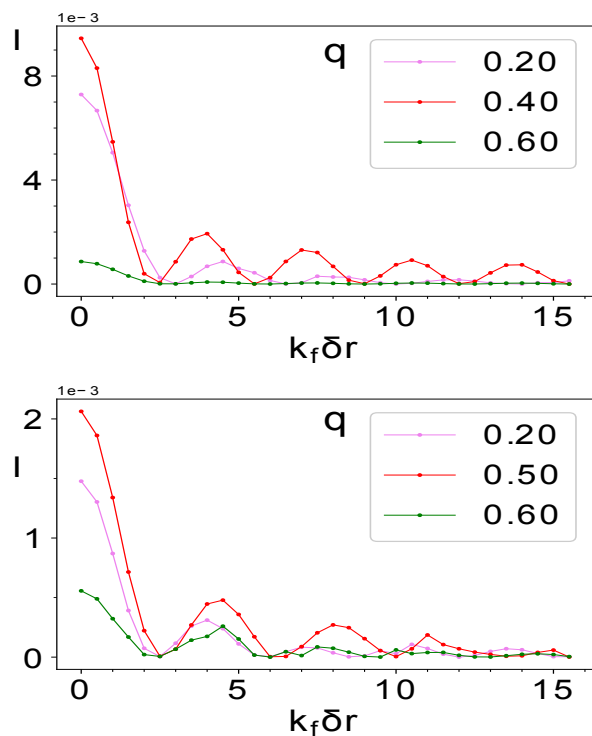


FIG. 5. Here we demonstrate two cases; pockets are of equal sizes (no doping in either pocket) in the upper panel whereas they are of different sizes for the bottom panel (here we have taken electron doped case but currents are same for hole doping and plots are for a given μ). For both the cases, different colors represent different amount of finite nesting for which currents have been plotted.

Having discussed the effect of doping at electron and hole pocket on beam current, we move on to discuss how the current behaves for non-zero nesting vector for different sizes of the hole and electron pocket. A non-zero nesting vector imply that if the electron pocket is situated at $(0, 0)$, the hole pocket is situated at $\mathbf{Q} + \mathbf{q}$ where $\mathbf{Q} = (\pi, \pi)$ and \mathbf{q} is called nesting vector. We also note that for non-zero \mathbf{q} , magnetic ordering is present along with superconducting ordering. In Fig. 5 upper panel we have taken electron and hole pocket to be of identical size i.e no doping and plotted current for representative value of \mathbf{q} . As can be seen, in this case also, the current varies in a non-linear fashion with respect to \mathbf{q} at given values of $k_f \delta r$. In the lower panel we have plotted the current for hole doped system (or electron doped system, the results is same) for various values of \mathbf{q} . This implies that in this case one pocket is bigger than the other. In this case also the beam splitter current is non-linear with respect to \mathbf{q} . In both the cases though we observe that as the magnitude of nesting vector increases, the beam current decreases, there is an oscillation for intermediate values of nesting vector. This oscillation arises due to same reason explained in previous section.

C. Oscillations of beam splitter current

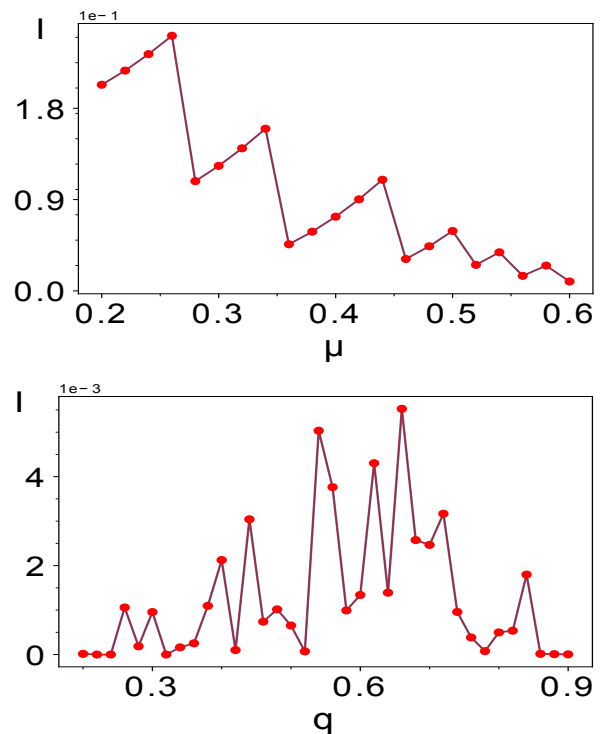


FIG. 6. In the upper panel Beam splitter current is plotted for different doping for $\mathbf{q}=0$ at a given $k_f \delta r$. In the lower panel beam splitter current is plotted for a fixed value of μ and $k_f \delta r$. In both the cases oscillations are observed. For discussions see text.

In the previous two sections we have explained that there are oscillations of beam splitter current. For a given $K_f \delta r$ the current depends in a non-linear way on the chemical potential or doping. To show this oscillations in a more transparent way, in Fig. 6, we plot the beam splitter current for different doping as well as for different nesting vector at some values of $k_f \delta r$. In the upper panel we plot the current for a given value of $k_f \delta r$ for $q = 0$. As we see the current decreases with respect to μ as expected but for intermediate ranges of μ current increases. This is the result of interdependence of ordering parameter on electron and hole pocket as discussed before. In the lower panel we plotted the beam splitter current for various values of \mathbf{q} for a given values of μ and $k_f \delta r$. We see that depending on the values of \mathbf{q} , current increases or decreases. We note that a finite \mathbf{q} represents a co-existence phase with simultaneous presence of magnetic and superconducting order parameter. The nature of oscillation is different than the previous case. Here we find a Gaussian-like distribution pointing out that there is optimal values of the nesting vector for which one obtains maximum beam splitter current.

V. DISCUSSION

To summarize we have proposed a Cooper pair beam splitter arrangement for Iron-pnictide superconductor which is known for hosting Cooper pairs responsible for superconducting property as well as inherent magnetic ordering. The co-existence of these two seemingly non-inclusive order parameters in a given material provides an interesting platform to investigate the consequences in a Cooper pair beam splitter current. We have considered various realistic situations found in actual materials such as zero nesting and finite nesting [27], equal and unequal size of hole and electron pockets etc. Most notably our finding indicates that in general the beam splitter current depends non-monotonically on electron μ_c and hole doping μ_f as well as on the magnitude of nesting vector $|\mathbf{q}|$. In all these cases there are a critical values for which the current is maximum. We believe that this fact might be useful in practical application such as switching and quantum gate applications. In all cases we find that the increase of magnetic ordering results in decrease of Cooper pair beam current as expected. This fact may be used to include the effect of external magnetic field on the beam current and find to the extent the current can be manipulated. The effect of external pressure may be useful to control the nesting vectors as found before [31]. Another useful way toward further investigation could be to study ferromagnetic proximity effect for quantum dots which could be useful to study the spin-spin correlations in

Iron-pnictides and its effect on beam-splitter current[32]. The effect of magnetic and non-magnetic impurity can be another aspect to look at and will be presented elsewhere.

ACKNOWLEDGMENTS

SM thanks Arijit Saha for useful discussions.

Appendix A: Appendixes-A

After diagonalisation and filling the negative energy states we obtain the following ground state energy, Corresponding minimum energy will be,

$$E_{min} = \sum_{kk's} -\frac{1}{\sqrt{2}} [\sqrt{(A + s\sqrt{B})} - 2\frac{\Delta_c \Delta_f}{V_{SC}} + 2\frac{m^2}{V_{SD}}] \quad (A1)$$

Where "s" can be +1 or -1; The function A, B are given below,

$$A = \Delta_c^2 + \Delta_f^2 + \epsilon_c^2 + \epsilon_f^2 + 2m^2, \quad (A2)$$

$$B = (\Delta_c^2 - \Delta_f^2 + \epsilon_c^2 - \epsilon_f^2)^2 + 4m^2((\Delta_c - \Delta_f)^2 + (\epsilon_c + \epsilon_f)^2) \quad (A3)$$

Appendix B: Eigenvector elements expression for current calculation

$$c_{k\sigma} = u_{1k}^c \gamma_{kq\sigma}^c + u_{1-k}^c \gamma_{-kq-\sigma}^{c\dagger} + u_{1k'}^f \gamma_{k'q\sigma}^f + u_{1-k'}^f \gamma_{-k'q-\sigma}^{f\dagger} \quad (B1)$$

$$c_{-kq-\sigma}^\dagger = u_{2k}^c \gamma_{kq\sigma}^c + u_{2-k}^c \gamma_{-kq-\sigma}^{c\dagger} + u_{2k'}^f \gamma_{k'q\sigma}^f + u_{2-k'}^f \gamma_{-k'q-\sigma}^{f\dagger} \quad (B2)$$

$$f_{k'\sigma} = u_{3k}^c \gamma_{kq\sigma}^c + u_{3-k}^c \gamma_{-kq-\sigma}^{c\dagger} + u_{3k'}^f \gamma_{k'q\sigma}^f + u_{3-k'}^f \gamma_{-k'q-\sigma}^{f\dagger} \quad (B3)$$

$$f_{-k'-\sigma}^\dagger = u_{4k}^c \gamma_{kq\sigma}^c + u_{4-k}^c \gamma_{-kq-\sigma}^{c\dagger} + u_{4k'}^f \gamma_{k'q\sigma}^f + u_{4-k'}^f \gamma_{-k'q-\sigma}^{f\dagger} \quad (B4)$$

Where $k' = k + q$; q is the ordering momentum and u are the elements of the eigen vectors of the Hamiltonian Eq. 12. The expressions for all the u can be written like following,

$$u_{iz}^p = \frac{a_{iz}^p}{\sqrt{\sum_{zp} (a_{iz}^p)^2}} \quad (B5)$$

We found a pattern in eigenvectors which compactly can be written as;

$$\begin{cases} d_{s_1} & = \Delta_+ \delta + \Delta_- (\zeta + s_1 E_i) \\ a & = \sqrt{(\Delta_+ \Delta_- - \delta \zeta)^2 + m^2 (\Delta_-^2 + \delta^2)} \\ a_{(i/i+1)k}^c & = (m^2 \delta + (\delta + \zeta + s_1 E_i) (-\Delta_+ \Delta_- + \delta \zeta + s_2 a)) / m d_{s_1} \\ a_{(i/i+1)-k}^c & = (\Delta_+ (\Delta_-^2 + \delta \zeta + s_2 a) - \Delta_- (\Delta_+^2 + \delta \zeta + s_2 a + m^2)) / m d_{s_1} \\ a_{(i/i+1)k}^f & = (\Delta_-^2 + \delta^2 + s_2 a + s_1 \delta E_i) / d_{s_1} \\ a_{(i/i+1)-k}^f & = 1 \end{cases}$$

provided, $s_2 = -1$ for $i = 1, 2$ $s_2 = +1$ for $i = 3, 4$ for all. $s_1 = +1$ for $i = 1, 3$ and $s_1 = -1$ for $i = 2, 4$; Note that here $E_{1,2} = \sqrt{A + \sqrt{B}}$, $E_{3,4} = \sqrt{A - \sqrt{B}}$

REFERENCES

-
- [1] J. J. Sakurai, Jim Napolitano, Modern Quantum Mechanics, Cambridge University Press, 3rd Edition(2020)
 - [2] Michael A. Neilson and Isaac L. Chuang Quantum Computations and Quantum Informations, Cambridge University Press (2003).
 - [3] David P. DiVincenzo, Fortschr. Phys. **48** (2000) 9-11, 771-783
 - [4] Ivan Djordjevic, Quantum Information Processing and Quantum Error Correction, 2012
 - [5] T. Bækkegaard, L. B. Kristensen, N. J. S. Loft, C. K. Andersen, D. Petrosyan & N. T. Zinner, Scientific Reports volume 9, Article number: 13389 (2019)
 - [6] Ashley Montanaro, npj Quantum Information volume 2, Article number: 15023 (2016)
 - [7] Walter Pötz Ulrich Hohenester Jaroslav Fabian, Quantum Coherence From Quarks to Solids, Springer
 - [8] T. van der Sar, Z. H. Wang, M. S. Blok, H. Bernien, T. H. Taminiau, D. M. Toyli, D. A. Lidar, D. D. Awschalom, R. Hanson & V. V. Dobrovitski, Nature volume **484**, pages82–86(2012)
 - [9] Tinkham, Michael (1996). Introduction to Superconductivity. Dover Publications.
 - [10] Yi Zhou, Kazushi Kanoda, and Tai-Kai Ng, Rev. Mod. Phys. **89**, 025003(2017)
 - [11] Lucile Savary and Leon Balents, 2017 Rep. Prog. Phys. **80**, 016502
 - [12] G Baskaran, Z Zou and P W Anderson, Sol. State Commun. **63** 973 (1987)
 - [13] A. Einstein, B. Podolsky, and N. Rosen, Phys. Rev. **47**, 777
 - [14] J.S. Bell, Speakable and unspeakable in quantum mechanics, Cambridge University Press, Cambridge, 1987
 - [15] A. Peres, Quantum theory: Concepts and methods, Kluwer, Dordrecht, 1993.
 - [16] Bei Zeng, Xie Chen, Duan-Lu Zhou, Xiao-Gang Wen, Quantum Information Meets Quantum Matter – From Quantum Entanglement to Topological Phase in Many-Body Systems, Springer, 2019(Book), arXiv:1508.02595
 - [17] Nicolas Laflorencie, Physics Report Volume 643, 1-59(2016)
 - [18] Andreas Osterloh, arXiv:0810.1240
 - [19] Patrik Recher, Eugene V. Sukhorukov, and Daniel Loss, Phys. Rev B. 63.165314 (2001)
 - [20] L.Hofstetter, S.Csonka, J.Nygaard and C.Schönenberger, Nature, Vol 461, 08432, 2009
 - [21] L. G. Herrmann, F. Portier, P. Roche, A. L. Yeyati, T. Kontos, and C. Strunk, Phys. Rev. Lett. **104**, 026801 (2010).
 - [22] SK Firoz Islam and Arijit Saha, Phys. Rev. B.96, 125406 (2017)
 - [23] Hideo Hosono, Akiyasu Yamamoto, Hidenori Hiramatsu, Yanwei Ma, Materials Today, Volume 21, Number 3, April 2018
 - [24] Hai-Hu Wen and Shiliang Li, Annu. Rev. Condens. Matter Phys. 2011. 2:121–40
 - [25] G. R. Stewart, REVIEWS OF MODERN PHYSICS, VOLUME 83, OCTOBER–DECEMBER 2011
 - [26] Qimiao Si, Rong Yu, Elihu Abrahams, Nature Rev. Mater. 1, 16017 (2016), arXiv:1604.03566
 - [27] A. V. Chubukov, V. Efremov and I. Eremin, Phys. Rev. B 78, 134512 (2008)
 - [28] A. B. Vorontsov, M. G. Vavilov and A. V. Chubukov, Phys. Rev. B 81, 174538 (2010)
 - [29] M. Sumetskiĭ, Phys. Rev. B **48**, 4586, 1993
 - [30] E. Merzbacher, Quantum Mechanics, 3rd ed. (Wiley, New York, 1998), Chap. 20
 - [31] Vladimir Cvetkovic and Zlatko Tesanovic, Phys. Rev. B **80**, 024512
 - [32] L. Hofstetter, A. Geresdi, M. Aagesen, J. Nygaard, C. Schönenberger, and S. Csonka, Phys. Rev. Lett **104**, 246804(2010)
 - [33] Michael R. Norman, The Challenge of Unconventional Superconductivity, 8 APRIL 2011 VOL 332 SCIENCE
 - [34] Y Bang and GR Stewart, 10.1088/1361-648X/aa564b
 - [35] D.J.Singh, Acta Physica Polonica A, 121, 2012
 - [36] F. Steglich, 10.1016/j.physc.2007.03.406.

- [37] A. Subedi, L. Zhang, D. J. Singh, and M. H. Du, Phys. Rev. B 78, 134514, 2008
- [38] I. I. Mazin, D. J. Singh, M. D. Johannes, and M. H. Du, Phys. Rev. Lett. 101, 057003, 2008
- [39] A. V. Chubukov, Physica C 469, 640, 2009
- [40] P. Samuelsson, E. V. Sukhorukov, and M. Büttiker, Phys. Rev. Lett. 91, 157002, 2003
- [41] P. Burset, W. J. Herrera, and A. Levy Yeyati, Phys. Rev. B 84, 115448, 2011
- [42] J. Rech, D. Chevallier, T. Jonckheere, and T. Martin, Phys. Rev. B 85, 035419, 2012
- [43] Koji Sato, and Yaroslav Tserkovnyak, Phys. Rev. B 90, 045419, 2014
- [44] Mattia Mantovani, Wolfgang Belzig, Gianluca Rastelli, and Robert Hussein, Phys. Rev. Research 1, 033098, 2019
- [45] M.K. Wu et al. Phys. Rev. Lett., 58 (9) (1987), p. 908